

The preferred stoichiometry of *c* subunits in the rotary motor sector of *Escherichia coli* ATP synthase is 10

Weiping Jiang, Joe Hermolin, and Robert H. Fillingame*

Department of Biomolecular Chemistry, University of Wisconsin Medical, School, Madison, WI, 53706

Edited by Paul D. Boyer, University of California, Los Angeles, CA, and approved February 15, 2001 (received for review September 5, 2000)

The stoichiometry of *c* subunits in the H⁺-transporting F_o rotary motor of ATP synthase is uncertain, the most recent suggestions varying from 10 to 14. The stoichiometry will determine the number of H⁺ transported per ATP synthesized and will directly relate to the P/O ratio of oxidative phosphorylation. The experiments described here show that the number of *c* subunits in functional complexes of F_oF₁ ATP synthase from *Escherichia coli* can be manipulated, but that the preferred number is 10. Mixtures of genetically fused cysteine-substituted trimers (*c*₃) and tetramers (*c*₄) of subunit *c* were coexpressed and the *c* subunits crosslinked in the plasma membrane. Prominent products corresponding to oligomers of *c*₇ and *c*₁₀ were observed in the membrane and purified F_oF₁ complex, indicating that the *c*₁₀ oligomer formed naturally. Oligomers larger than *c*₁₀ were also observed in the membrane fraction of cells expressing *c*₃ or *c*₄ individually, or in cells coexpressing *c*₃ and *c*₄ together, but these larger oligomers did not copurify with the functional F_oF₁ complex and were concluded to be aberrant products of assembly in the membrane.

The ATP made during oxidative and photo phosphorylation is synthesized by closely related enzymes located in the inner membrane of mitochondria, the thylakoid membrane of chloroplasts, and the plasma membrane of eubacteria (1). Recent evidence supports a rotary mechanism for ATP synthesis in which proton-transport-coupled rotation of an oligomeric ring of *c* subunits in the membrane is coupled to rotary movement of subunit γ between alternating catalytic sites in the $\alpha_3\beta_3$ sector of the enzyme (refs. 2–8; Fig. 1). The proton-motive force is thought to drive rotation of the *c*-ring by a transport mechanism by using half channels that connect the aspartyl-61 proton-binding site of subunit *c* in the middle of the membrane to the aqueous compartments on either side of the membrane. After H⁺ binding from the entrance half channel at the *a*₁*b*₂ stator, the *c* subunit carrying the proton would rotate nearly 360° before encountering the H⁺ exit channel on the opposite side of the membrane. In such a mechanism, the number of H⁺ transported per revolution of the *c* oligomer would equal the number of subunit *c* in the ring. The number of subunit *c* would also determine the H⁺/ATP stoichiometry (i.e., H⁺ transported per ATP synthesized) and directly relate to the P/O ratio for oxidative phosphorylation, a fundamental parameter of biology (9).

The number of *c* subunits in F_o is controversial. Direct measurements of subunit ratios in *Escherichia coli* F_oF₁, after growth of cells on radioactive amino acids, indicated a range of 10 ± 1 *c* per 3 $\alpha\beta$ pairs in the purified F_oF₁ complex or 12 *c* per 3 $\alpha\beta$ in the membrane fraction in which F_oF₁ was overproduced (10). More recently, genetically fused subunit *c* were generated by insertion of a loop between the C-terminal residue of transmembrane helix-2 (TMH-2) of the first subunit and the N-terminal residue of TMH-1 of the next subunit (11). The genetically fused *c*₂ dimers and *c*₃ trimers were both active, which suggested that the stoichiometry was a multiple of two and three. Further, after introduction of Cys into these fused *c*₂ and *c*₃ subunits and crosslinking via disulfide bond formation, oligo-

meric ladders that maximized at *c*₁₂ (i.e., *c*₂ × 6 or *c*₃ × 4) were observed, which suggested a likely maximal stoichiometry of 12 *c* per oligomeric ring. Two recent observations led us to reexamine the stoichiometry question. First, Stock *et al.* (12) reported a 3.9-Å-resolution electron density map of a crystallized mitochondrial F₁/*c*-oligomer subcomplex, lacking the other subunits of F_o, in which there were only 10 *c* subunits. Second, Seelert *et al.* (13) reported an SDS-purified *c*-oligomer preparation from chloroplasts, which, according to atomic force microscopic analysis, organizes into a ring of 14 subunits after reconstitution into lipid bilayers. Explanations for these differences include the possibility of variable stoichiometry in different species, the possible loss of subunits on crystallization of the mitochondrial subcomplex (12), the possible association of *c* subunits into unnatural oligomeric rings during extraction and reconstitution (13), or the possibility that the expression of fused *c* subunits in *E. coli* forced an unnatural arrangement of the *c*-oligomer (11). In the experiments reported here, we show that the stoichiometry of *c* subunits in a functional F_oF₁ of *E. coli* can be varied, but that the preferred number is 10.

Experimental Procedures

Construction and Expression of Fused *c*₃ and *c*₄ Subunits. Genetically fused trimers and tetramers of subunit *c* containing the I30C substitution in the first and last subunit were constructed by using restriction enzymes cutting at the following positions of the *atp* operon, with the numbering system of Walker *et al.* (14): *Pst*I(1561), *Bam*HI(1727), *Bsr*GI(1911), *Ava*I(1976), *Hpa*I(2162), *Eco*O109I(2342), *Pvu*II(2376), and *Sph*I(3216). The I30C substitution occurs at nucleotides 1973–1975 just before the *Ava*I(1976) site. The *Pst*I/*Ava*I fragment from the plasmid encoding *c*₁(I30C) (11) was ligated with the 205-bp *Ava*I/*Bsr*GI fragment from plasmid pC2A (11), which codes the *c*₂ dimer (the fragment coding respectively the C-terminal region from the first unit, the linker, and the N-terminal region of the second unit from the middle of the *c*₂ dimer), and ligated into the *Pst*I/*Bsr*GI sites of plasmid pNOC (15) to generate plasmid *c*₂(I30C-1) with I30C substituted in the first or N-terminal subunit. The 681-bp *Pst*I/*Ava*I fragment from a partial digest of plasmid *c*₂(I30C-1) and 205-bp *Ava*I/*Bsr*GI fragment of plasmid C2A were ligated into the *Pst*I/*Bsr*GI sites of plasmid *c*₁(I30C) to generate plasmid *c*₃(I30C-1/I30C-3) with I30C substitutions in the first and last subunits of the trimer. The 886-bp *Pst*I/*Bsr*GI fragment and 524-bp *Bsr*GI/*Hpa*I fragment prepared from a partial digests of plasmid *c*₃(I30C-1/I30C-3) were ligated into the *Pst*I/*Hpa*I sites of plasmid pNOC (15) to generate plasmid *c*₄(I30C-1/I30C-4)

This paper was submitted directly (Track II) to the PNAS office.

Abbreviation: ACMA, 9-amino-6-chloro-2-methoxyacridine.

*To whom reprint requests should be addressed at: Department of Biomolecular Chemistry, 1300 University Avenue, University of Wisconsin Medical School, Madison, WI 53706. E-mail: rhfillin@facstaff.wisc.edu.

The publication costs of this article were defrayed in part by page charge payment. This article must therefore be hereby marked "advertisement" in accordance with 18 U.S.C. §1734 solely to indicate this fact.

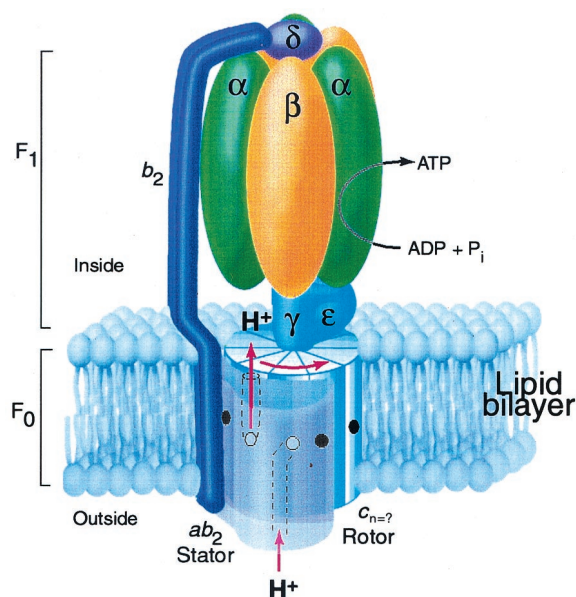


Fig. 1. Rotary model for ATP synthase based on the subunit composition of the *E. coli* enzyme (8). The F_1 portion of the complex is bound at the cytoplasmic face of the membrane. The proton-motive force drives rotation of a ring composed of c subunits, the number (n) of which is uncertain. Protons enter the assembly through a periplasmic inlet channel and bind to the Asp⁶¹ carboxylate (open circle) of a subunit c at the a_1b_2 stator interface. The protonated binding site then moves from the stator interface into the lipid phase of the membrane, and after n steps the proton is released at an outlet channel on the F_1 -binding side of the membrane. The γ and ϵ subunits remain fixed to the top of a set of c subunits so that rotation of the c oligomer also drives rotation of subunit γ within the $\alpha_3\beta_3$ hexamer of F_1 to alternatively promote ADP + P_i binding and ATP product release in the β catalytic subunits. The b_2 and δ subunits of the stator hold the $\alpha_3\beta_3$ subunits in a fixed position as the γ subunit turns inside them to drive ATP synthesis. The coupled reaction catalyzed by the complex is reversible so that ATP hydrolysis will drive proton transport in the reverse of the direction shown. This figure is modified from ref. 8.

with I30C substitutions in the first and last subunit of the c_4 tetramer. The c_3 (I30C-1/I30C-3) and c_4 (I30C-1/I30C-4) plasmids, which in addition code the a , b , and δ subunits of F_0F_1 , proved capable of complementing a chromosomal strain from which the a , c , b , and δ subunits were deleted from the chromosome (11), i.e., the transformants were capable of slow growth on succinate minimal medium via oxidative phosphorylation. Derivatives of plasmid pACYC184 (16) carrying the gene for “ c -only” (pCO plasmids) were constructed by ligating the *Bam*HI/*Hpa*I fragments from the c_3 (I30C-1/I30C-3) or c_4 (I30C-1/I30C-4) plasmids into the *Bam*HI/*Hin*CII sites of plasmid pACYC184. These “ c -only” plasmids are designated pCOc3(I30C) and pCOc4(I30C) in the text. Whole operon plasmids were generated in a derivative of plasmid pBR322 (17) in which the *rop* gene had been deleted (18). In this plasmid, the *atp* operon from *Hind*III(870)-*Nde*I(9531) is ligated between the *Hind*III and *Nde*I sites of the pBR322 vector. The c_3 (I30C) and c_4 (I30C) genes were inserted as *Eco*O109I fragments between an *Eco*O109I site in the vector, 49 base pairs before the vector *Hind*III site, and the *Eco*O109I(2342) site in the *atp* operon. These “whole operon” plasmids are designated pWOc3(I30C) and pWOc4(I30C) in the text.

General Methods. Membranes were prepared in 50 mM Tris-HCl, pH 7.5/5 mM MgCl₂/10% (vol/vol) glycerol [TMG buffer: 50 mM Tris-HCl, pH 7.5/5 mM MgCl₂/10% (v/v) glycerol] by rupture of cells in a French press (19). ATPase-coupled proton

pumping was measured indirectly by the quenching of 9-amino-6-chloro-2-methoxyacridine (ACMA) fluorescence (18). Membranes were suspended in assay buffer at a protein concentration of 250 μ g/ml and ACMA added to 0.3 μ g/ml. To initiate the quenching response, ATP was added to 0.92 mM. To terminate the quenching response, the protonophore SF6847 was added to 0.25 μ M. Membrane ATPase activity was measured as described (18), with 0.5% lauryldimethylamine oxide included in the assay buffer to remove the inhibitory ϵ subunit. To crosslink subunits, membranes at 5 mg/ml in TMG buffer were treated with 100 μ M I₂ in TMG buffer for 1 h at 22°C. The reaction was stopped by addition of Na₂S₂O₃ and *N*-ethylmaleimide to 0.4 and 20 mM, respectively, and the membranes collected by centrifugation.

SDS gel electrophoresis and immunoblotting, by using an “ECL System” (Amersham Pharmacia Biotech.) for blot development, was carried out as described in Jones *et al.* (15). Enhanced chemiluminescence (ECL)-developed immunoblots were scanned in several instances to more quantitatively estimate the proportions of different oligomeric species. In these cases, multiple gel lanes were scanned after different development times to ensure that the scanned density was within the linear limits of the scanner. Control experiments were run to determine whether the efficiency of electrophoretic transfer varied for different sized oligomers. When the electrophoretic transfer time was altered from the routine time of 90 min to 45 or 135 min, all subunits from c_3 through c_{12} transferred with nearly maximal transfer occurring by 90 min. The proportion of larger subunits did increase somewhat between 45 and 90 min but then remained constant at the 135-min interval. We interpret this as indicating that electrophoretic transfer of subunits from the SDS gel to the polyvinylidene difluoride membrane is essentially complete at 90 min, and that the blots accurately sample the total protein content of the gel.

Purification and Reconstitution of F_0F_1 Complex. The complete F_0F_1 ATPase complex was purified by slight modifications of the procedure used by Foster and Fillingame (10, 19). Treated membranes were first suspended at 5 mg/ml and washed with 1 mM Tris-H₂SO₄, pH 8, buffer containing 0.5 mM Na₂EDTA, 10% (vol/vol) glycerol and 6 mM *p*-aminobenzamidine to remove extrinsic membrane proteins. Washed membranes were resuspended at 12–15 mg/ml in 50 mM Tris-HCl, pH 7.5/1 mM MgSO₄/10% (vol/vol) methanol buffer containing 1 mM phenylmethylsulfonyl fluoride, 6 mM *p*-aminobenzamidine, and solid KCl then added to a final concentration of 1 M. The F_1F_0 complex was then extracted by addition of Na-deoxycholate and Na-cholate to final concentrations of 0.5%. After 10 min on ice, the suspension was centrifuged at 186,000 $\times g$ for 60 min at 4°C and 0.4 ml of the soluble supernatant solution applied to a 4.4-ml linear 10–35% (vol/vol) glycerol gradient prepared in 10 mM Mes/10 mM tricine/1 mM MgCl₂ buffer made pH 7 with NaOH, which also contained 0.1% phosphatidylcholine (Sigma no. P3644) and 0.28% Na-deoxycholate. The gradients were centrifuged at 237,000 $\times g_{avg}$ for 4 h at 4°C in a SW55Ti Beckman rotor. The gradients were fractionated into 0.5-ml fractions. The peak fractions shown in Figs. 4–6 correspond to those showing maximal dicyclohexylcarbodiimide-sensitive ATPase activity (19) and, after reconstitution into liposomes, exhibiting maximal ATP-driven quenching of ACMA fluorescence. Gradient fractions were reconstituted into acetone-precipitated soybean phosphatidylcholine (Sigma no. P3644) by the dialysis method of Kagawa and Sone (20). Aliquots of 0.2 ml were added to 8 mg of dried phosphatidylcholine and Na-cholate, Na-deoxycholate, and Na₂EDTA added to final concentrations of 1.6%, 0.8%, and 2 mM, respectively, in a final volume of 0.3 ml. Dialysis was carried out at 4°C versus 10 mM Tricine-NaOH, pH 8/2.5 mM MgSO₄/0.2 mM Na₂EDTA buffer.

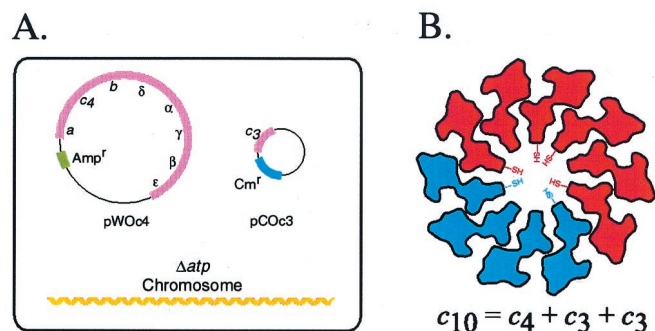


Fig. 2. Strategy for testing the preferred number of subunit *c* in *E. coli* F_0F_1 complex. (A) System used for coexpression of c_3 (I30C) and c_4 (I30C) substituted proteins in one cell. The eight genes of the *atp* (ATP synthase) operon are deleted from the chromosome of the cell shown. In the scheme shown, the c_4 subunit is expressed from a pBR322-derived plasmid carrying genes for the whole *atp* operon (pWOC4), with transformant cells selected on the basis of plasmid-encoded ampicillin resistance (Amp^r). The c_3 subunit is expressed by itself from a pACYC184-derived plasmid with transformant cells being selected for via chloramphenicol resistance (Cm^r). (B) Coexpression of c_3 (I30C) and c_4 (I30C) in the same cell should lead to formation of a c_{10} decamer if that is the preferred structure in F_0 . The figure shows the positions of the I30C-substituted cysteine in the first and last subunit of the c_3 trimer and c_4 tetramer. The approximate shape of a cross section of subunit *c* at the position of the I30C substitution is indicated (21). Cys–Cys crosslinking is expected to yield c_6 , c_7 , and c_{10} products.

Results

Test of Preferred Stoichiometry by Coexpression of c_3 and c_4 Fused Subunits.

In the key experiment described here, we have coexpressed genetically fused c_3 trimers and c_4 tetramers in the same *E. coli* cell (Fig. 2A). If mixing of the subunits occurs in the membrane of these cells, it should be possible to form a c_{10} oligomer (Fig. 2B). To detect formation of the possible c_{10} oligomer, we have introduced a Cys at position 30 into transmembrane helix-1 of the first and third unit of the c_3 trimer and the first and fourth unit of the c_4 tetramer (Fig. 2B). The approximate position of the Cys-30 substitution at the hub of the *c*-ring, based on the oligomeric model of Dmitriev *et al.* (21), is indicated in Fig. 2B. If a c_{10} oligomer forms on mixing of c_3 and c_4 in the same membrane, then c_6 , c_7 , and c_{10} crosslinked products should be observed on crosslinking (Fig. 2B). If c_{12} is the predominant oligomeric species, then crosslinked products corresponding to c_6 , c_8 , c_9 , and c_{12} should predominate, and the c_7 and c_{10} species should be missing.

In the configuration shown in Fig. 2A, the c_4 tetramer is expressed from a pBR322 derived plasmid encoding all of the genes of the F_0F_1 complex [pWOC4(I30C)], where pWO denotes “whole operon” plasmid, and the c_3 trimer is expressed by itself from a pACYC184-derived plasmid [pCOC3(I30C)], where pCO denotes “*c* only” plasmid. On growth of these cells, both c_3 and c_4 were incorporated into the membrane with the amounts of c_3 exceeding the amount of c_4 by a $1.6 \pm 0.1/1$ molar ratio, based on scans ($n = 11$) of immunoblots of membrane fractions (see *Experimental Procedures* for controls on quantitation). When the subunits were expressed in the opposite configuration, i.e., pWOC3(I30C)/pCOC4(I30C), the c_3 (I30C) and c_4 (I30C) subunits were expressed in an equimolar ratio, i.e., $1.0 \pm 0.1/1$ ratio ($n = 9$ scans).

Function of Fused c_3 and c_4 Subunits. The ATPase-coupled proton-pumping activity of F_0F_1 made from the c_3 (I30C) and c_4 (I30C) fused products is shown in Fig. 3. In both cases, ATP hydrolysis resulted in formation of a ΔpH , as indicated by the quenching of ACMA fluorescence, but the c_3 (I30C) species of enzyme was

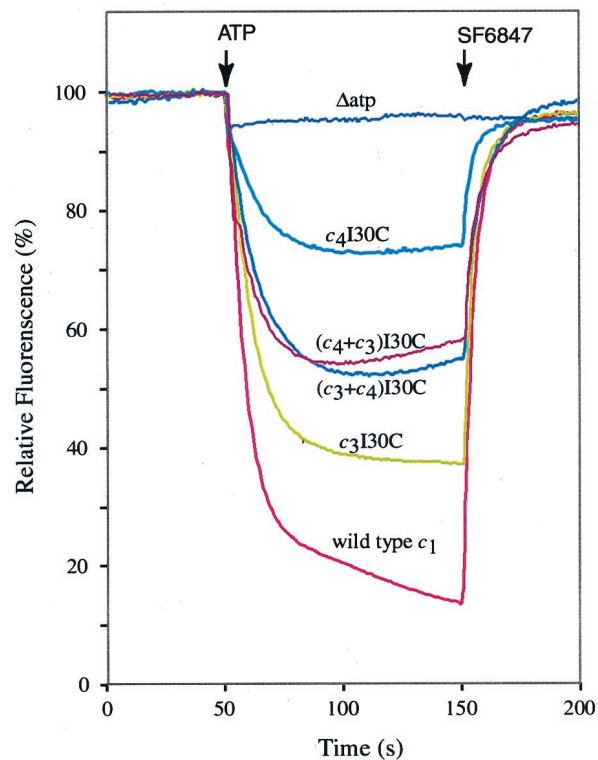


Fig. 3. ATP-driven proton translocation with membrane vesicles from cells expressing c_3 or c_4 by themselves, or cells coexpressing c_3 and c_4 . Coexpression in the pWOC4/pCOC3 and pWOC3/pCOC4 configurations are indicated as $(c_4 + c_3)$ I30C and $(c_3 + c_4)$ I30C, respectively. The quenching of ACMA fluorescence was used as an indicator the pH gradient established by ATPase-coupled proton pumping. At the times indicated, ATP was added to 0.92 mM and, to terminate the quenching response, the protonophore SF6847 was added to 0.25 μM to make the membranes proton permeable.

considerably more active than the c_4 (I30C) species. Activity was intermediate in membranes in which both types of subunits were expressed. Membranes prepared from cells expressing both subunit types exhibited somewhat greater ATPase activity than cells expressing c_3 (I30C) or c_4 (I30C) only, and the activity was inhibited by dicyclohexylcarbodiimide (Table 1). ATPase activity measured in the presence of the detergent lauryldimethylamine oxide is the best measure of the total amount of F_0F_1 incorporated into the membrane. The overexpression of *c* subunits, or coexpression of c_3 and c_4 , may thus facilitate greater assembly of the F_0F_1 complex.

Crosslinking Generates c_{10} Oligomers. To detect formation of the possible c_{10} oligomer, we introduced a Cys at position 30 into

Table 1. Membrane ATPase activities from cells expressing c_3 and c_4 fused subunits

Plasmids expressed	ATPase activity*		Inhibition by DCCD†
	–LDAO	+LDAO	
pWOC3(I30C)	0.61	3.48	73%
pWOC4(I30C)	0.81	4.40	70%
pWOC3(I30C)/pCOC4(I30C)	1.20	5.45	72%
pWOC4(I30C)/pCOC3(I30C)	1.45	7.10	55%

*Membrane ATPase activity measured with and without 0.5% LDAO, which activates F_1 ATPase by disassociation of the inhibitory ϵ subunit. Activity expressed in units of $\mu mol min^{-1} mg^{-1}$.

†Membrane ATPase activity was measured after preincubation of membranes at 10 $\mu g/ml$ in ATPase assay buffer with 50 μM DCCD for 20 min at 22°C.

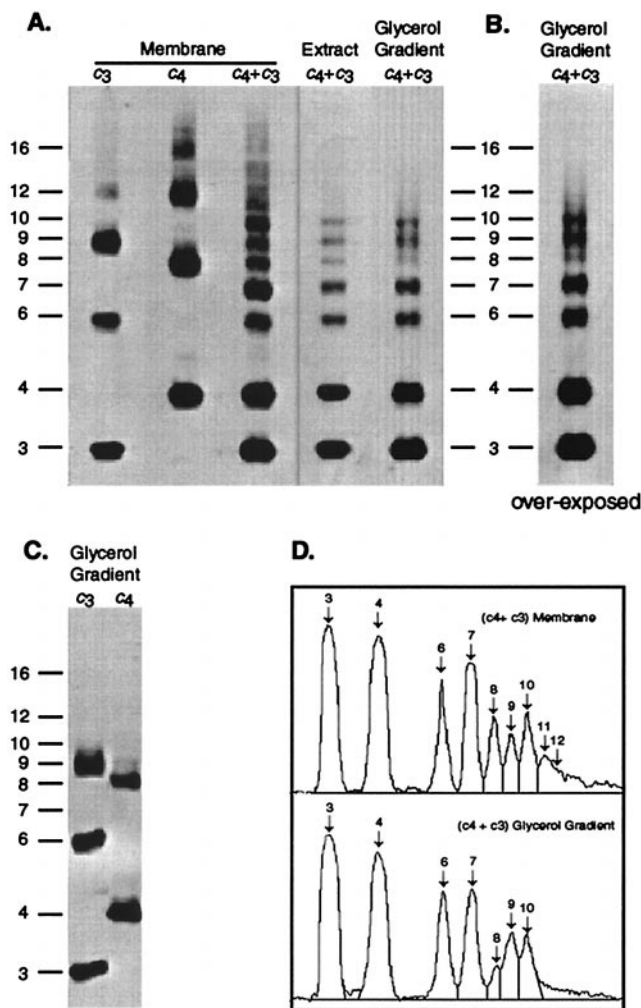


Fig. 4. Crosslinked products generated in membranes from cells expressing c_3 (I30C) and c_4 (I30C) subunits. All samples were prepared after crosslinking of membranes with I_2 . The oligomeric size of the crosslinked product is indicated on the vertical axis. (A) Membranes prepared from cells expressing pWoc3(I30C) or pWoc4(I30C) individually or cells expressing both and pWoc4(I30C) and pCoc3(I30C). The deoxycholate/cholate extract and glycerol gradient purified F_0F_1 fractions from the pWoc4(I30C)/pCoc3(I30C) membranes is also shown. (B) Glycerol gradient fraction shown in A after prolonged development. (C) Glycerol gradient F_0F_1 fractions prepared from the c_3 or c_4 membranes shown in A. (D) Scan of lanes of ($c_4 + c_3$) membrane and glycerol gradient shown in A.

transmembrane helix-1 of the first and third unit of the c_3 trimer and the first and fourth unit of the c_4 tetramer (Fig. 2B). The Cys substitution at this position was chosen because the monomeric I30C subunit c forms a high yield of dimers, i.e., >95% (15). Further, dimerization of the c_1 (I30C) subunits resulted in minimal reduction of ATPase-coupled proton pumping and must therefore result in minimal structural perturbations.[†] The crosslinking of coexpressed subunits is shown in Fig. 4. The first two lanes show the crosslinking of c_3 (I30C) or c_4 (I30C), respectively, when each was expressed individually from the pBR322-derived whole operon plasmids, i.e., pWoc3(I30C) and pWoc4(I30C). Subunits were detected by immunoblotting of the

[†]Treatment of c_1 (I30C) membranes with 1.5 mM Cu^{+2} -(phenanthroline)₂ resulted in a 34% diminution of the ATPase coupled ACMA quenching response under conditions giving rise to 95% dimer formation. The equivalent treatment of wild-type membranes resulted in a similar 36% reduction of the ACMA quenching response.

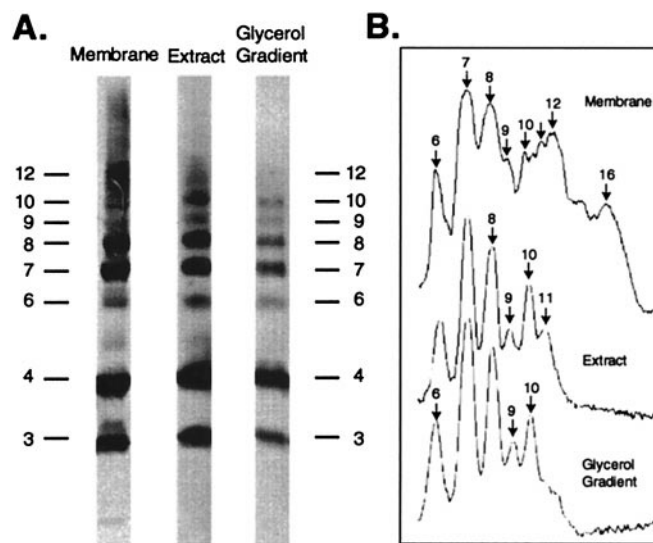


Fig. 5. Crosslinked products generated in membranes from cells expressing both the pWoc3(I30C) and pCoc4(I30C) plasmids. Membranes were treated with I_2 and the F_0F_1 complex extracted and purified by glycerol gradient centrifugation as described in the text. (A) Lanes from immunoblot. (B) Scan of crosslinked products $\geq c_6$ in the three lanes shown.

plasma membrane fraction. With the c_3 membrane, c_6 and c_9 were the predominant crosslinked products with a smaller amount of c_{12} also detected. With the c_4 membrane, the predominant products were c_8 and c_{12} , but a significant amount of c_{16} was also observed. When the c_3 (I30C) and c_4 (I30C) subunits were coexpressed from the pWoc4(I30C)/pCoc3(I30C) configuration (shown in Fig. 2A) and membranes crosslinked, distinct products corresponding to c_6 , c_7 , c_8 , c_9 , c_{10} , c_{11} , and c_{12} were observed. Note that the c_7 signal is slightly more intense than either c_6 or c_8 .

A significantly different pattern was observed when the F_0F_1 complex was extracted from these membranes, by using a cholate and deoxycholate detergent mixture, and then purified by glycerol density gradient centrifugation. Crosslinked oligomers of sizes greater than c_{10} were not observed as is most apparent from the overexposed lane of the purified glycerol gradient fractions (Fig. 4B), where there is no hint of oligomers greater than c_{10} . Note that the predominant dimeric species in the purified F_0F_1 fraction was clearly c_6 ($c_3 + c_3$) and c_7 ($c_3 + c_4$), with lesser amounts of c_8 ($c_4 + c_4$) being found (Fig. 4B and D). Nearly equal amounts of trimeric c_9 ($c_3 + c_3 + c_3$) and trimeric c_{10} ($c_3 + c_3 + c_4$) were observed, so the tendency to form rings of 9 or 10 seems to be nearly identical. The F_0F_1 complex was also prepared from crosslinked membranes in which c_3 and c_4 were expressed individually (Fig. 4C). In the case of c_3 , the largest crosslinked oligomer corresponded to c_9 . In the case of c_4 , the largest crosslinked oligomer corresponded to c_8 . We conclude that the crosslinked oligomers in membranes of sizes greater than c_{10} are not likely to be components of a functional F_0F_1 complex but rather may be an artifact of aberrant assembly in the membrane.

When coexpressed in the configuration opposite to that shown in Fig. 2A and Fig. 4, i.e., with plasmids pWoc3(I30C) and pCoc4(I30C), the c_3 and c_4 subunits were incorporated into the membrane in an equimolar ratio. After crosslinking in this case, c_7 and c_8 were the predominant dimeric products and lesser amounts of c_6 dimer seen (Fig. 5A). Prominent trimeric products of c_9 , c_{10} , c_{11} , and c_{12} were apparent in the membrane fraction. However, the c_9 and c_{10} trimers were again preferentially extracted and purified with the F_0F_1 fraction (Fig. 5A and B). In

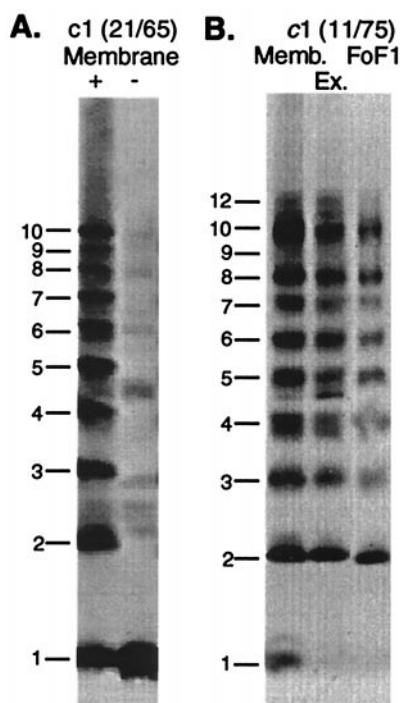


Fig. 6. Cu(II)-phenanthroline catalyzed crosslinking of monomeric subunit *c* with double Cys substitutions. (A) Membrane fraction of $c_1(\text{Cys}^{21}/\text{Cys}^{65})$ with (+) and without (-) crosslinking. (B) The crosslinked membrane, deoxycholate/cholate extract, and purified F_0F_1 from the $c_1(\text{Cys}^{11}/\text{Cys}^{75})$ mutant are shown. Crosslinking was carried out as described (15).

this case, a distinct c_{11} trimer was also detected in the solubilized detergent extract but was much less evident in the purified F_0F_1 fraction (Fig. 5B). Although it is possible that trace quantities of c_{11} and c_{12} are present in the F_0F_1 fraction, the key point is that most of oligomeric species $> c_{10}$ are lost as the complete enzyme is purified. Membranes from cells coexpressing c_3 and c_4 in the two configurations show equivalent ATP-driven ACMA quenching activity (Fig. 3). Because relatively less c_6 and c_9 , and relatively more c_7 and c_{10} , were found in the pWoc3(I30C)/pCoc4(I30C) membranes, most of the activity can be attributed to the c_{10} form of the enzyme.

Monomeric Subunit *c* Forms a c_{10} Oligomer in F_0F_1 . The conclusion that c_{10} is the preferred stoichiometry actually agrees well with previous crosslinking experiments with a doubly Cys substituted c_1 monomers, where crosslinking usually generated products maximizing at the position of the c_{10} oligomer (15). Such an example is shown in Fig. 6A with the $\text{Cys}^{21}/\text{Cys}^{65}$ doubly substituted c_1 monomer. In the study of Jones and Fillingame (11), one doubly Cys-substituted c_1 protein (from the $\text{Cys}^{11}/\text{Cys}^{75}$ mutant) generated crosslinked products in the membrane that appeared to maximize at c_{12} . As a followup to the experiments reported here, the crosslinked F_0F_1 complex was purified from $c_1(\text{Cys}^{11}/\text{Cys}^{75})$ membranes. Products migrating at positions $> c_{10}$ were not observed in the F_0F_1 fraction (Fig. 6B); again, these products appear to be minor artifacts of assembly, formed in the membrane, but not assembling into a functional F_0F_1 complex.

Discussion

From the experiments reported here, we conclude that the preferred stoichiometry of *c* subunits in the oligomeric ring of *E. coli* F_0 is 10. The experiments also indicate that *c*-oligomers composed of nine or eight subunits exhibit at least partial

function. Although crosslinked products composed of more than 10 *c* subunits were observed in membranes, these oligomers did not copurify with the functional F_0F_1 complex and are probably artifacts of assembly. In the key experiment done here, we used genetically fused c_3 and c_4 subunits to test whether 10 or 12 was the preferred stoichiometry. After coexpression of the c_3 and c_4 subunits, crosslinking generated a prominent c_{10} product, which was the maximum sized product seen in the purified F_0F_1 complex. Oligomers larger than c_{10} were observed in the membrane fraction, but these did not extract with or copurify with the active F_0F_1 complex. We envision occasional assembly of oligomeric rings with > 10 *c* subunits in the membrane, perhaps because of expression of c_3 and c_4 in nonstoichiometric ratios, but also envision that these larger rings do not assemble with subunits *a* or *b* to form a functional F_0 or bind F_1 . The differences in the structure of rings composed of 9–12 subunits are probably quite minor.[‡] However, a cell very likely regulates the stoichiometry at a fixed number under normal physiological conditions, as discussed below.

The c_3 and c_4 subunits were coexpressed in two configurations, which resulted in slightly different ratios of subunit incorporation into the membrane and slight differences in the relative amounts of different types of crosslinked dimers and trimers in the membrane. Importantly, in either expression configuration, c_7 was the most prominent dimeric product and c_{10} the most prominent trimeric product in purified F_0F_1 , supporting the conclusion that c_{10} is the preferred species. The relative amounts of c_6 and c_8 dimer varied depending on whether c_3 or c_4 was expressed in excess. Because c_3 or c_4 , when expressed individually, form oligomers in purified F_0F_1 composed of c_9 ($c_3 + c_3 + c_3$) or c_8 ($c_4 + c_4$) only (see Fig. 4C), the membrane fraction of cells coexpressing c_3 and c_4 is likely to contain a mixture of F_0F_1 composed of c_8 , c_9 , c_{10} , and possibly c_{11} rings. However, on purification of F_0F_1 , the only well defined trimers seen were c_9 and c_{10} . Other oligomers, if present, could be present only in trace amounts.

One might argue that the *c*-ring formed from the genetically fused subunits is itself unnatural. However, the crosslinking data with monomeric subunits presented here also support a preferred stoichiometry of c_{10} versus c_{12} . In the case of the $c_1(\text{Cys}^{21}/\text{Cys}^{65})$, crosslinking in the membrane maximized at c_{10} with no hint of a c_{12} product (Fig. 6A). With $c_1(\text{Cys}^{11}/\text{Cys}^{75})$ membranes, some c_{12} crosslinked product was observed in the membrane but not in the purified F_0F_1 complex (Fig. 6B). That crosslinked products with masses $> c_{10}$ do not copurify with functional complex suggests they are aberrant assembly products formed only in the membrane. The formation of oligomers $> c_{10}$ in the membrane clearly depends on the position of the double Cys substitutions in the protein. In the case of $c_1(\text{Cys}^{11}/\text{Cys}^{75})$, the 11 and 75 regions of the protein are clearly more flexible (15, 18) and may account for minor amounts of aberrant product formation. The position of the genetically introduced cysteine is clearly critical in the formation of different oligomers as c_9 products are formed in $\text{Cys}^{21}/\text{Cys}^{65}$ and other membranes (15) but not with the $\text{Cys}^{11}/\text{Cys}^{75}$ -substituted protein.

Despite the clear formation of a c_{10} crosslinked product in purified F_0F_1 from either fused or monomeric subunits, one

[‡]In Dmitriev *et al.* (21), a *c* oligomer of 12 subunits was modeled on the basis of 21 intersubunit distance constraints and the then assumed stoichiometry of 12 subunit *c*. By using the same approach, an oligomeric ring with 10 subunits has now been modeled (O. Y. Dmitriev, personal communication; see ref. 22). The changes in the model are relatively minor and predictable, e.g., the diameter of the ring decreases from ≈ 60 to 55 Å. The packing interactions between subunits change very little. One of the important predicted interactions between subunits in the ring is between the Asp^{61} side chain at the front face of one subunit *c* and the Ala^{24} side chain at the back face of the preceding subunit (21). The distance between the Asp^{61} carboxylate carbon and Ala^{24} β -carbon changes from 4.2 Å in the c_{12} model to 4.4 Å in the c_{10} model. Similarly, only minor structural differences would be expected in the packing of a c_{10} versus c_9 oligomer.

might suggest that c_9 is the preferred stoichiometry on the basis of the experiment shown in Fig. 3. The c_3 membrane vesicles show greater proton-pumping activity than membrane vesicles in which c_3 and c_4 are coexpressed. However, the low activity of the c_4 enzyme, also present in the c_3/c_4 hybrid membranes, should be considered in any accounting of an average lower total activity. ATP-driven ACMA quenching activity was observed with pWoc3(I30C)/pCoc4(I30C) membranes, which matched that of the pWoc4(I30C)/pCoc3(I30C) membranes. Because lesser amounts of c_9 crosslinked product were observed in the pWoc3(I30C)/pCoc4(I30C) membranes (Fig. 5), most of the activity observed can be attributed to the c_{10} species of enzyme.

The mechanism by which the cell regulates assembly of the oligomer is of interest. The cell would be at a bioenergetic disadvantage if it were to assemble functional mixtures of c oligomers with different c stoichiometries. At thermodynamic equilibrium for ATP synthesis, the free energies of the proton-motive force ($\Delta\bar{\mu}H^+$)/ F and phosphorylation potential ($\Delta G_p = \Delta G'^{\circ} + RT \ln[ATP]/[ADP][Pi]$) are in balance, i.e. $(H^+/ATP)\Delta\bar{\mu}H^+ = \Delta G_p$. With a mixture of two enzymes, e.g., c_9 and c_{10} , at least one of the enzymes would not be in thermodynamic equilibrium with $\Delta\bar{\mu}H^+$. Depending on the displacement from equilibrium, the F_0F_1 complex with the higher c_n stoichiometry would preferentially synthesize ATP, whereas the complex with the lower c_n stoichiometry would preferentially hydrolyze ATP, resulting in an uncoupled system. It seems likely that cells precisely control c -oligomer assembly to prevent such mixtures and the potential problem of uncoupling.

The experiments presented here do not answer the question of whether there are differences in subunit c stoichiometry in different species. Indeed, the presence of a natural subunit c trimer in the *Methanococcus jannaschii* archaeobacterial ATP synthase argues for such diversity (23), although the absence of a proton-binding carboxylate (equivalent to Asp⁶¹) in the first unit of the trimer suggests that the mechanism of rotary catalysis, if applicable, might be more complicated. The conclusion that 10 is the preferred stoichiometry in the c oligomer of *E. coli* does support the suggestion of a c_{10} oligomer in yeast mitochondria, a suggestion based on the crystal structure of an F_1c_{10} subcomplex (12). A mitochondrial ATP synthase with a c_{10} oligomer would use 3.3 H^+ per ATP synthesized. If the consensus values for proton pumping by the mitochondrial respiratory chain are correct (9, 24), an H^+/ATP stoichiometry of 3.3 is quite compatible with the P/O ratios measured for mitochondrial oxidative phosphorylation by Hinkle *et al.* (25) and would suggest a P/O ratio of 2.3 for NADH-linked substrates and 1.4 for succinate versus the classical textbook values of 3 and 2, respectively (9). The H^+/ATP pumping ratio predicted for a c_{10} oligomeric ring also fits well with a thermodynamically determined ratio of $H^+/ATP = 3$, estimated for whole cells of *E. coli* by measurements of $\Delta\bar{\mu}H^+$ and ΔG_p (26).

We thank Ms. Wilmara Salgado-Pabon and Ms. Krista L. Porter for assistance in some of the experiments reported. This research was supported by National Institutes of Health Grant GM23105.

- Boyer, P. D. (1997) *Annu. Rev. Biochem.* **66**, 717–749.
- Noji, H., Yasuda, R., Yoshida, M. & Kinosita, K., Jr. (1997) *Nature (London)* **386**, 299–302.
- Duncan, T. M., Bulygin, V. V., Zhou, Y., Hutcheon, M. L. & Cross, R. L. (1995) *Proc. Natl. Acad. Sci. USA* **92**, 10964–10968.
- Sabert, D., Engelbrecht, S. & Junge, W. (1996) *Nature (London)* **381**, 623–625.
- Sambongi, Y., Iko, Y., Tanabe, M., Omote, H., Iwamoto-Kihara, A., Ueda, I., Yanagida, T., Wada, Y. & Futai, M. (1999) *Science* **286**, 1722–1724.
- Pänke, O., Gumbiowski, K., Junge, W. & Engelbrecht, S. (2000) *FEBS Lett.* **472**, 34–38.
- Junge, W. (1999) *Proc. Natl. Acad. Sci. USA* **96**, 4735–4737.
- Fillingame, R. H. (1999) *Science* **286**, 1687–1688.
- Nelson, R. H. & Cox, M. M. (2000) *Lehninger Principles of Biochemistry* (Worth, New York), 3rd Ed.
- Foster, D. L. & Fillingame, R. H. (1982) *J. Biol. Chem.* **257**, 2009–2015.
- Jones, P. C. & Fillingame, R. H. (1998) *J. Biol. Chem.* **273**, 29701–29705.
- Stock, D., Leslie, A. G. W. & Walker, J. E. (1999) *Science* **286**, 1700–1705.
- Seelert, H., Poetsch, A., Dencher, N. A., Engel, A., Stahlberg, H. & Müller, D. J. (2000) *Nature (London)* **405**, 418–419.
- Walker, J. E., Saraste, M., Gay, J. E. (1984) *Biochim. Biophys. Acta* **768**, 164–200.
- Jones, P. C., Jiang, W. & Fillingame, R. H. (1998) *J. Biol. Chem.* **273**, 17178–17185.
- Cohen, A. C. Y. & Cohen, S. N. (1978) *J. Bacteriol.* **134**, 1141–1148.
- Bolivar, F., Rodriguez, R. L., Greene, P. J., Betlach, M. C., Heynecher, H. L., Boyer, H. W., Crosa, J. H. & Falkow, S. (1977) *Gene* **2**, 95–113.
- Jones, P. C., Hermolin, J., Jiang, W. & Fillingame, R. H. (2000) *J. Biol. Chem.* **275**, 31340–31346.
- Foster, D. L. & Fillingame, R. H. (1979) *J. Biol. Chem.* **254**, 8230–8236.
- Kagawa, Y. & Sone, N. (1979) *Methods Enzymol.* **55**, 364–372.
- Dmitriev, O. Y., Jones, P. C. & Fillingame, R. H. (1999) *Proc. Natl. Acad. Sci. USA* **96**, 7785–7790.
- Fillingame, R. H., Jiang, W. & Dmitriev, O. Y. (2000) *J. Bioenerg. Biomemb.* **32**, 433–439.
- Ruppert, C., Kavermann, H., Wimmers, S., Schmid, R., Kellermann, J., Lottspeich, F., Huber, H., Stetter, K. O. & Müller, V. (1999) *J. Biol. Chem.* **274**, 25281–25284.
- Nicholls, D. G. & Ferguson, S. J. (1992) *Bioenergetics 2* (Academic, London).
- Hinkle, P. C., Kumar, M. A., Resetar, A. & Harris, D. L. (1991) *Biochemistry* **30**, 3576–3582.
- Kashket, E. R. (1982) *Biochemistry* **21**, 5534–5538.